Cavitation study of a pump-turbine at turbine mode with critical cavitation coefficient condition

J Wang[1], D Yang[1], J W Xu[1], J T Liu[2], L Jiao[*]

[1] Institute of Naval Architecture and Ocean Engineering, Zhejiang University, China
[2]Beijing Institute of Control Engineering, Beijing, China
*Corresponding author: Tel.: +8613093767519;

E-mail: jiaolei@zju.edu.cn

Abstract. To study the cavitation phenomenon of a pump-turbine at turbine mode when it ran at the critical cavitation coefficient condition, a high-head model pump-turbine was disperse using hexahedron grid. Three dimensional, steady cavitating flow was numerically studied using SST k-ω model. It is confirmed that ZGB cavitation model and SST k-ω model are useful ways to study the two-phase cavitation flow in pump-turbine. Mass flow inlet and pressure outlet were specified at the casing inlet and draft tube outlet, respectively. The static pressure was set according to the cavitation coefficient. The steady cavitating flows at critical cavitation coefficient condition were analysed. The cavitation area in the runner was investigated. It was found that the pressure of the suction on the blade surface was decreasing gradually with the decrease of the cavitation coefficient. In addition, the vortex flow in the draft tube was observed at the critical cavitation coefficient. It was found that the vortex flow appeared at the center of the draft tube inlet with the decreasing of the cavitation coefficient. Compared with the experimental data, the simulation results show reasonable agreement with the experimental data.

1. Introduction

The cavitation is one of important phenomenon in a pump-turbine at turbine model. With the development of the cavitation flow, the cavitation bubble would collapse and perish, which would cause material erosion, structure wreck, vibration and noise. But due to hydraulic machine was in low speed state, even if it had cavitation wreck, the wreck was not very critical, that trigger the short of the cavitation research [1]. In recent years, the pump-turbine develop quickly, big capacity, high head and high speed gradually become the main developing aspect gradually. Finally, the condition of the blade wreck, efficiency reduces, device destroys, noise and vibration would aggravate gradually. So the cavitation problem of the pump-turbine has become one of the important research topics of domestic and foreign academia and engineering.

With the rapid development of computing technology in recent years, the simulation by the computational fluid dynamics can get some useful results in the engineering, except experimental method [2, 3]. In recent year, a lot of research about the mechanism of the cavitation form had been done. Wang Ya-yun [4] researched the unsteady hydrodynamic characteristics of a 2D cavitating hyrdrofoil and the evolution of cloud cavition, and compared the phenomenon of shedding and break-off sheet cavitation and behaviour of cloud cavitation by using the Reynolds Averaged Navier-stokers

equations, Detached Eddy Simulation and Large Eddy Simulation. The numerical results of 2D LES show that the generation and evolution of the vortex near the wake of sheet cavity in the primary reason of break-off sheet cavitation, and the reentrant jet occurs only after the break of the sheet cavity. This research about the cavitation mechanism Wu [5] studied the unsteady cavitating turbulent flow with two different models and found that the mixture model could fit the experimental data compared with the single-phase model. Nishi [6] analysed the influence of the draft tube flow and the pressure fluctuation of the draft tube caused by the different cavitation coefficient by the experiment, the pressure fluctuation frequency is almost invariant until the cavitation coefficient is less than the certain value that would magnitude the pressure fluctuation.

However, the analysis of the instability of a pump-turbine at critical cavitation coefficient hasn't yet been reported. In present paper, a two-phase cavitation model was used to predict the cavitating turbulent flow in a model Francis pump-turbine by numerical simulation. The distribution of the cavitation area in the runner was investigated.

The main parameters of the model mixed flow water turbine studied are showed in Table.1. D1 denotes the diameter of the runner outlet in turbine mode, Z denotes the number of the blades, Zs and Zg denote the number of the stay vanes and the guide vanes respectively, n denotes the velocity of the runner and H denotes the head of the test. The structure of the turbine is showed in the Figure.1.

Table 1. The main parameters of the model mixed flow water turbine.

Parameter	Value
D(m)	0.26
Zs	20
H(m)	50
Zg	20
Z	9

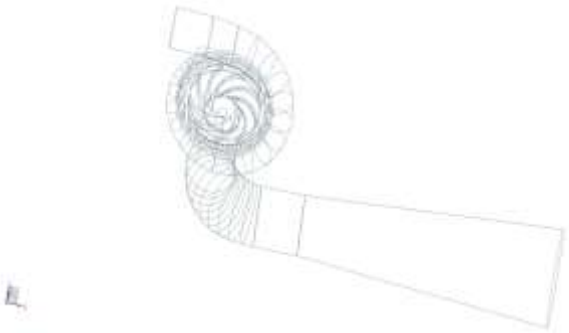

Figure 1. Figure with profile of the turbine.

2. Numerical method

2.1. Cavitation model

Zwart-Gerber-Belamri model was used to model cavitation in the pump-turbine. It was compatible with turbulence model well. It considered the evaporation and the condensation to control the equation. The evaporation and the condensation was included are defined as

When $p \le p_b$,

$$R_e = F_{vap}\frac{3\alpha_V(1-\alpha_V)\rho_v}{R_B}\left[\frac{2}{3}\left(\frac{P_V-P}{\rho_l}\right)\right]^{1/2} \tag{1}$$

When $p > p_b$,

$$R_e = F_{cond}\frac{3\alpha_V\rho_v}{R_B}\left[\frac{2}{3}\left(\frac{P_V-P}{\rho_l}\right)\right]^{1/2} \tag{2}$$

Where the diameter of the bubble was 1μm, $F_{vap} = 50$ and $F_{cond} = 0.01$ which represented factors for vaporization and condensation respectively; ρ_v was the saturated vapour pressure; ρ_l was the density of the fluid; the void fraction of the nuclei was 5×10^{-4}.

2.2. Turbulence model

The SST k-ω model developed by Menter [7] was adopted for the calculation of the unsteady cavitating flow in the pump-turbine. It combined k-ω model in the near-wall region and k-ε model in the far field.

$$\rho_m\frac{\partial k}{\partial t}+\rho_m u_j\frac{\partial k}{\partial x_j}=\frac{\partial}{\partial x_j}\left[(\mu+\sigma_k\mu_T)\frac{\partial k}{\partial x_j}\right]-\beta^*\rho_m k\omega+P_k \tag{3}$$

$$\rho_m\left(\frac{\partial \varepsilon}{\partial t}+u_j\frac{\partial \omega}{\partial x_j}\right)=\frac{\partial}{\partial x_j}\left[(\mu+\sigma_k\mu_T)\frac{\partial k}{\partial x_j}\right]+2(1-F_1)\sigma_{\omega 2}\frac{\rho_m}{\omega}\frac{\partial k}{\partial x_j}\frac{\partial \omega}{\partial x_j} \tag{4}$$
$$-\rho_m\left(\alpha S^2-\beta\omega^2\right)$$

Where,

$$P_K = \min\left(\tau_{ij}\frac{\partial u_i}{\partial x_j},10\beta^*k\omega\right),$$

$$F_1 = \tanh\left\{\left\{\min\left[\max\left(\frac{\sqrt{k}}{\beta^*\omega y},\frac{500\mu}{\rho_m y^2\omega}\right),\frac{4\sigma_{m2}}{CD_{km}y^2}\right]\right\}^4\right\},$$

$$CD_{k\omega} = \max\left(2\rho\sigma_{\omega 2}\frac{1}{\omega}\frac{\partial k}{\partial x_i}\frac{\partial \omega}{\partial x_i},10^{-10}\right),$$

Coefficients are chosen as $\alpha = 5/9$, $\beta = 0.075$, $\beta^* = 0.09$, $\sigma_k = 0.85$, $\sigma_{\omega 1} = 0.5$, $\sigma_{\omega 2} = 0.5$.

2.3. Boundary conditions

In the algorithm, the physical timescale was 0.001s. The head was specified 50m. The rotating speed of the runner was set by the function. Mass flow at casing inlet was specified at turbine mode. The outlet condition was used the value of static pressure. The outlet pressure was specified according to

the function. The advection scheme was specified high resolution and the turbulence numeric was specified first order.

Three cavitation efficient operation conditions in the optimum operation condition and partial load condition were showed in Table.2, which were set by the cavitation coefficient.

Table 2. Calculation conditions for three cases.

Case	Cavitation coefficient	*n(rpm)*	Mass flow inlet(kg*m3/s)	*Pressure outlet(Pa)*
Optimum	0.12	1061	0.252	632162.0
Optimum	0.08	1061	0.252	42897.0
Optimum	0.06	1061	0.252	32764.5
Partial load (82%)	0.12	1378	0.207	632162.0
Partial load (82%)	0.08	1378	0.207	42897.0
Partial load (82%)	0.06	1378	0.207	32764.5
Partial load (70%)	0.12	1445	0.167	63162.0
Partial load (70%)	0.08	1445	0.167	42897.0
Partial load (70%)	0.06	1445	0.167	32764.5

3. Result and discussion

3.1. Hydraulic performance

The steady state performances under three different rotate speed and mass flow at inlet was simulated and the results were compared with test data, as shown in Figure.2. It can be seen from the Figure.2 that the numerical results meets well with the test results and the numerical method could predict the hydraulic characteristics accurately.

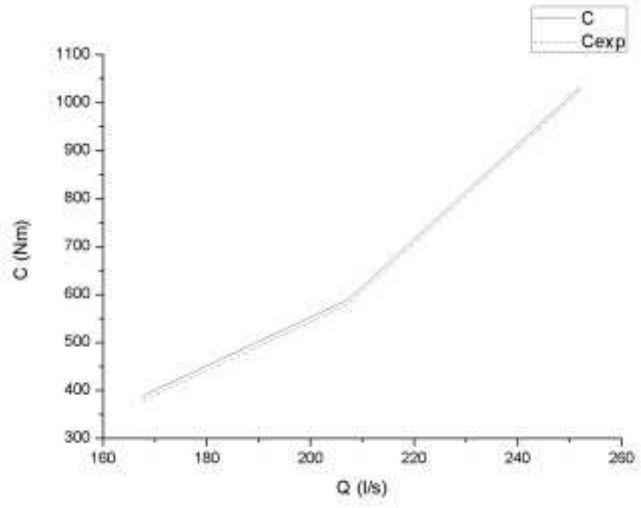

Figure 2. Figure with steady state Q-C performance at different speed.

3.2. Cavitation performance

Figure.3 – Figure.11 show the pressure distribution at the runner blade at different cavitation coefficient and at different load. It can be seen from the figures that, the low-pressure area is obviously exited on the suction side of the blade surface. With the decrease of the cavitation coefficient, the pressure of the low-pressure areas is decreasing gradually. And with the load decreasing, the pressure of the low-pressure areas is increasing at the same cavitation coefficient.

Figure.12 – Figure.20 show the vapour volume on the runner blade at different cavitation coefficient of the optimum load and at different load. It can be learned that, the obvious cavitation area is existed when the cavitation coefficient is at 0.06. Because of the pressure decrease of the low-pressure area, the vapour occurs while the pressure of the area is lowered than the saturate pressure of the water. Compared with the condition at the same cavitation coefficient, the cavitation area at the optimum load is larger than which at the 82% load and the 70% load.

The pressure distribution at the draft tube is showed at the Figure.21 – Figure.29. Figure.21-Figure.23 shows the cavitation coefficient at 0.12, 0.08 and 0.06 when it is at the optimum load, Figure.24 – Figure.26 when at the 80% partial load and Figure.27 – Figure.29 when at the 70% partial load. It can be learned that, compared with the same load, the pressure of the center area of the draft tube inlet is decreased gradually with the decreasing of the cavitation coefficient. And when the cavitation coefficient is lowered to 0.06, whatever the load is, the vortex flow occurs at the draft tube. In addition, compared with the different load when the cavitation coefficient is at 0.06, it show that the cavitation area is bigger at the 80% partial load than which at the 72% partial load and optimum load. And it has occurred a vortex at the 80% partial load. If the vortex frequency is same with the blade rotating frequency, it would lead to the strongly vibration, which will bring about huge damage.

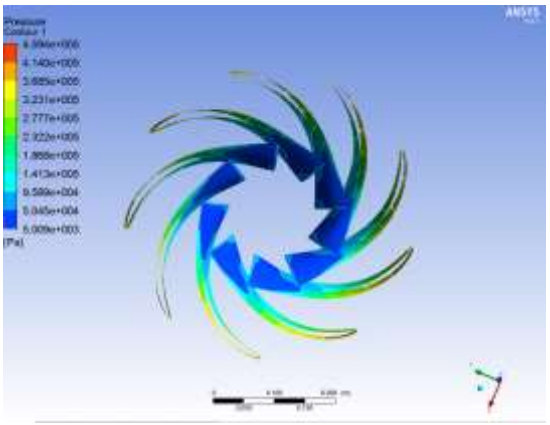

Figure 3. Pressure distribution at runner blade, Optimum, Cavitation coefficient 0.12.

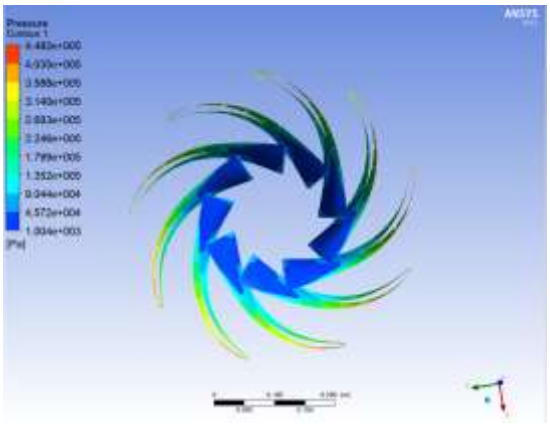

Figure 4. Pressure distribution at runner blade, optimum, Cavitation coefficient 0.08.

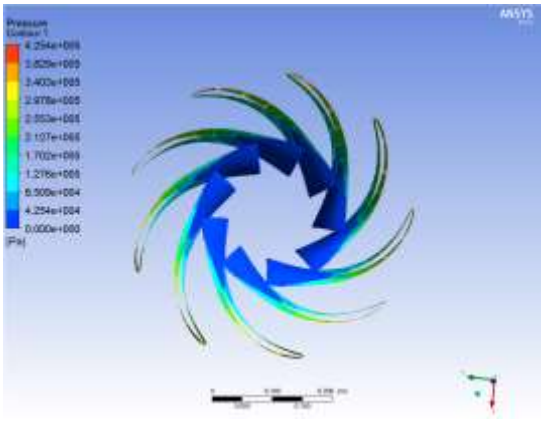

Figure 5. Pressure distribution at runner

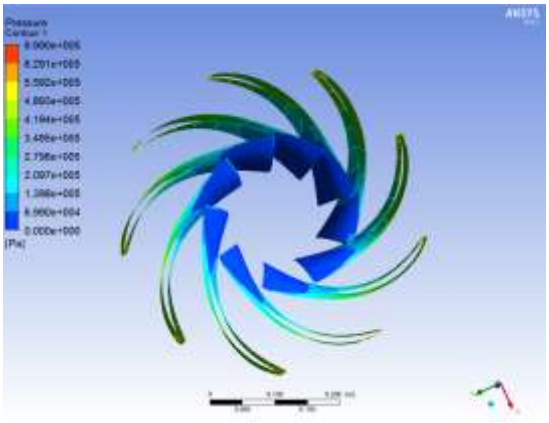

Figure 6. Pressure distribution at runner

blade, Optimum, Cavitation coefficient 0.06.

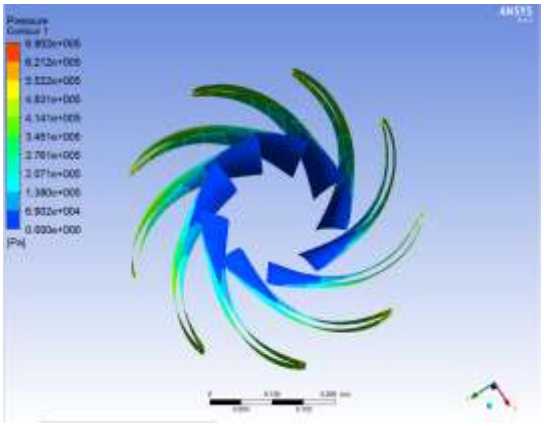

Figure 7. Pressure distribution at runner blade, Load 82%, Cavitation coefficient 0.08.

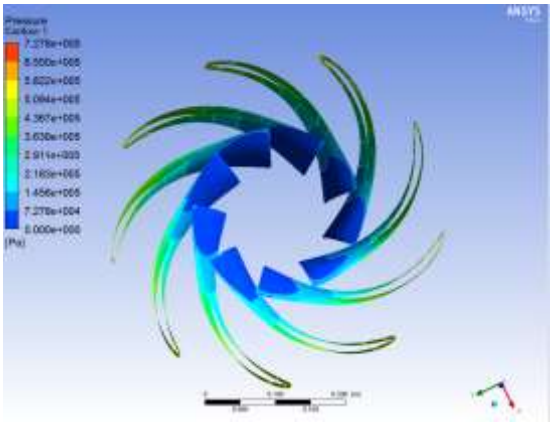

Figure 9. Pressure distribution at runner blade Load 70%, Cavitation coefficient 0.12.

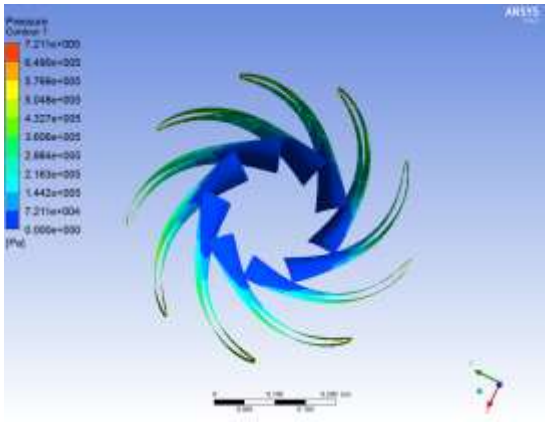

Figure 11. Pressure distribution at runner blade, Load 70%, Cavitation coefficient 0.06.

blade, Load 82%, Cavitation coefficient 0.12.

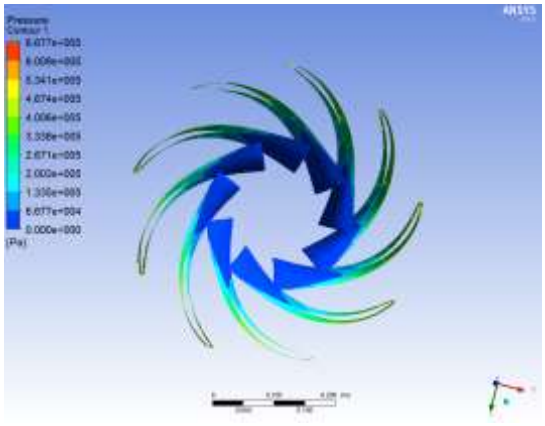

Figure 8. Pressure distribution at runner blade, Load 82%, Cavitation coefficient 0.06.

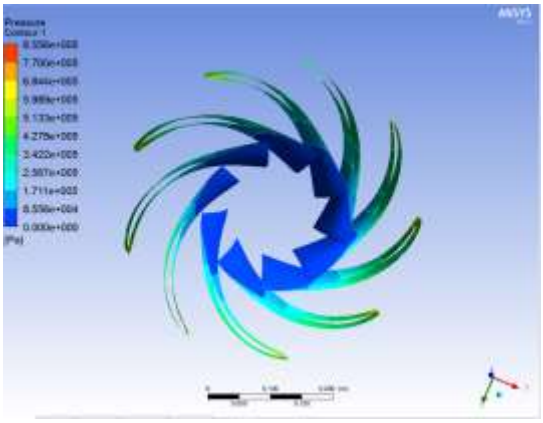

Figure 10. Pressure distribution at runner blade, Load 70%, Cavitation coefficient 0.08.

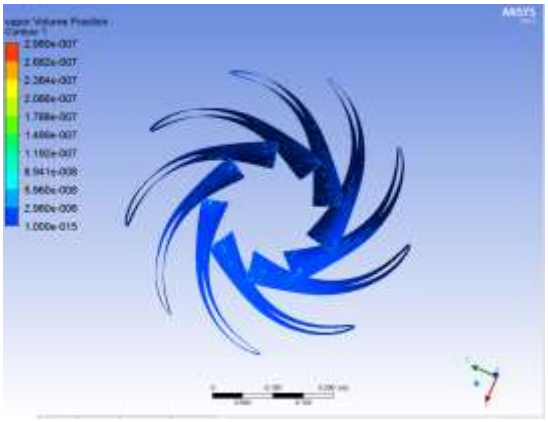

Figure 12. Vapour volume distribution at runner blade, Optimum, Cavitation coefficient 0.12.

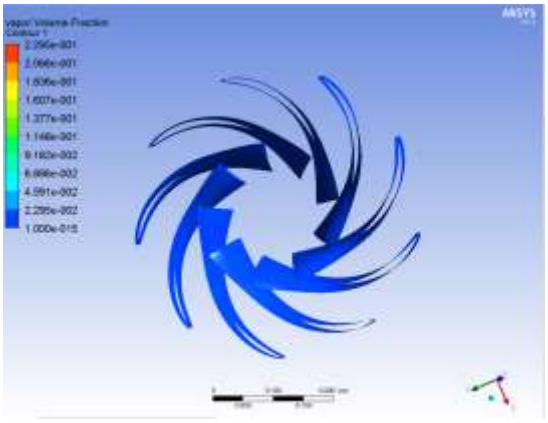

Figure 13. Vapour volume distribution at runner blade, Optimum, Cavitation coefficient 0.08.

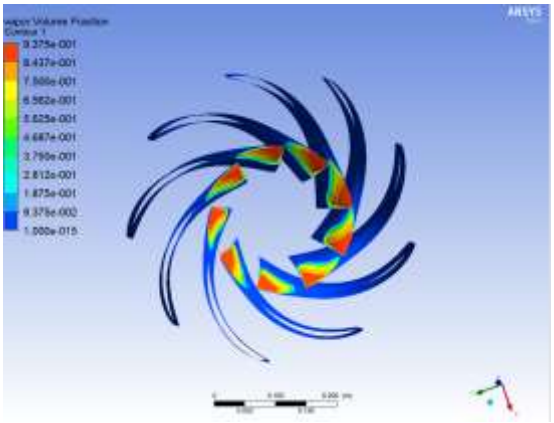

Figure 14. Vapour volume distribution at runner blade, Optimum, Cavitation coefficient 0.06.

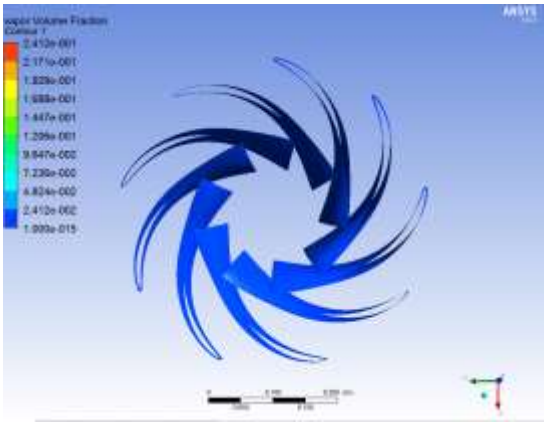

Figure 15. Vapour volume distribution at runner blade, Load 82%, Cavitation coefficient at 0.12).

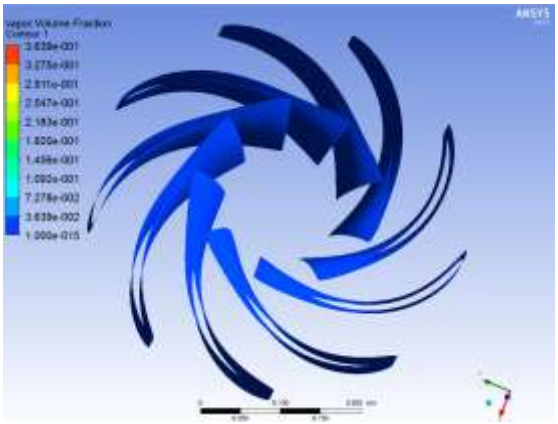

Figure 16. Vapour volume distribution at runner blade, Load 82%, Cavitation coefficient at 0.08.

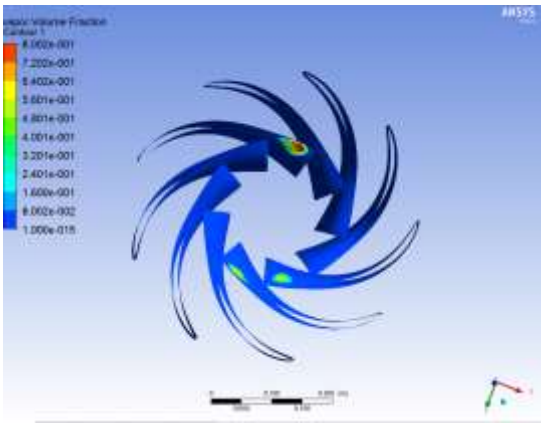

Figure 17. Vapour volume distribution at runner blade, Load 82%, Cavitation coefficient 0.06.

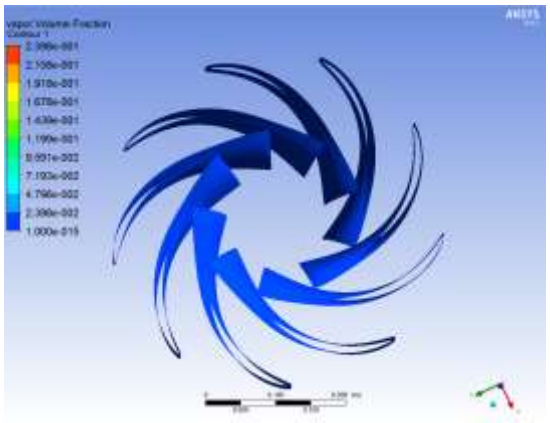

Figure 18. Vapour volume distribution at runner blade, Load 70%, Cavitation coefficient 0.12.

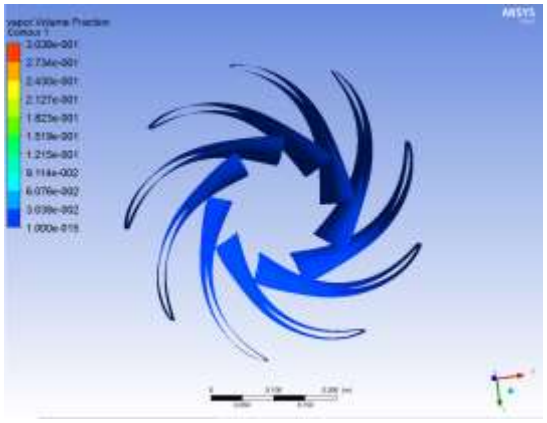

Figure 19. Vapour volume distribution at runner blade, Load 70%, Cavitation coefficient 0.08.

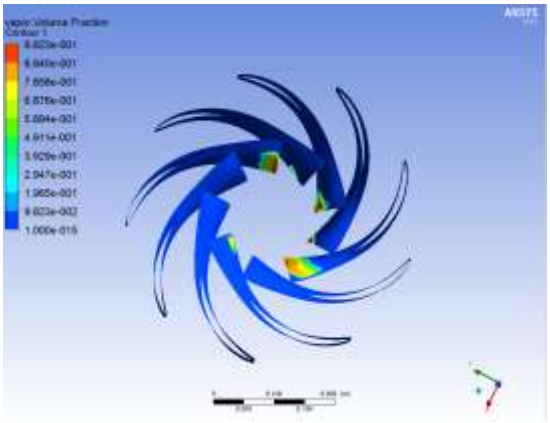

Figure 20. Vapour volume distribution at runner blade, Load 70%, Cavitation coefficient 0.06.

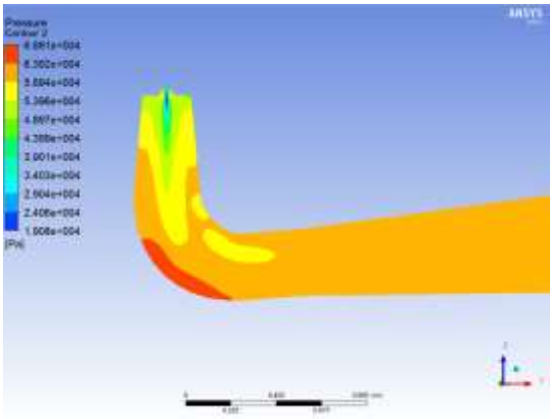

Figure 21. Vapour volume distribution at draft tube, Optimum, Cavitation coefficient 0.12.

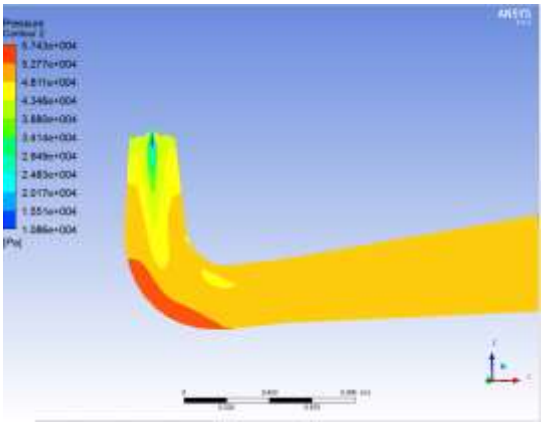

Figure 22. Vapour volume distribution at draft tube, Optimum, Cavitation coefficient 0.08.

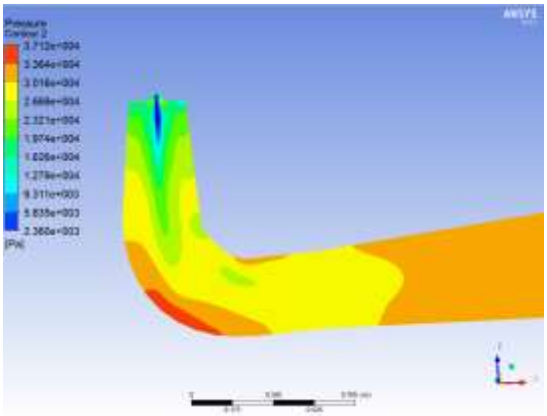

Figure 23. Vapour volume distribution at draft tube, Optimum, Cavitation coefficient 0.06.

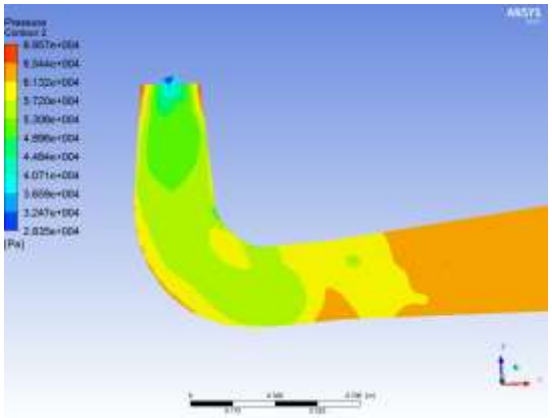

Figure 24. Vapour volume distribution at draft tube Load 82%, Cavitation coefficient 0.12.

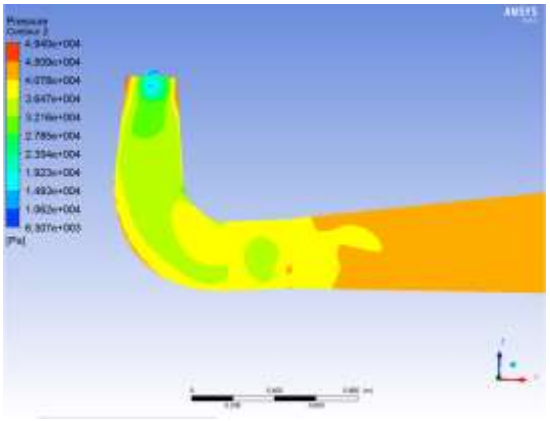

Figure 25. Vapour volume distribution at draft tube, Load 82%, Cavitation coefficient 0.08.

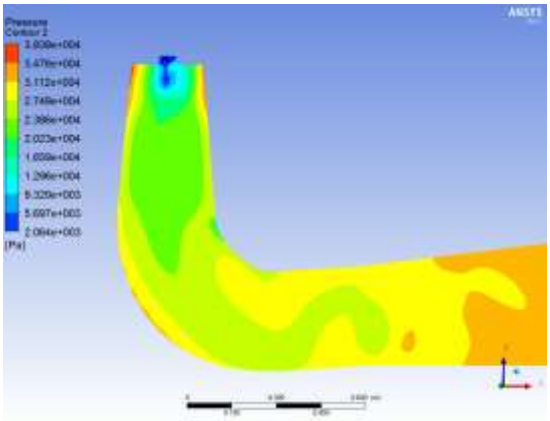

Figure 26. Vapour volume distribution at draft tube, Load 82%, Cavitation coefficient 0.06.

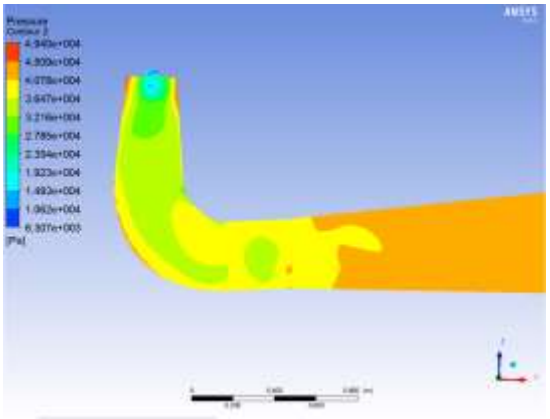

Figure 27. Vapour volume distribution at draft tube, Load 70%, Cavitation coefficient 0.12.

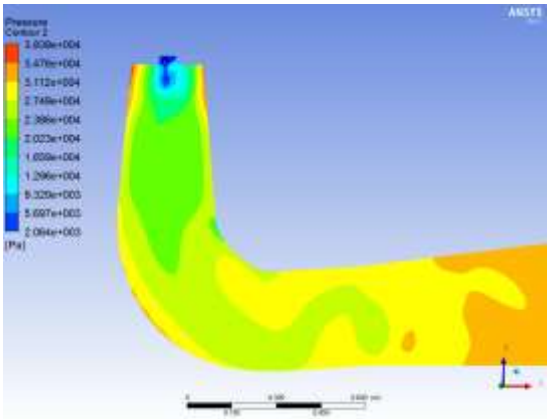

Figure 28. Vapour volume distribution at draft tube, Load 70%, Cavitation coefficient 0.08.

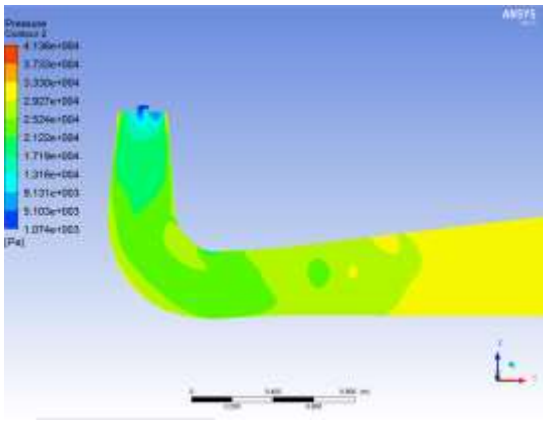

Figure 29. Vapour volume distribution at draft tube, Load 70%, Cavitation coefficient 0.06.

4. Conclusions

In this paper, a kind of numerical method for cavitation performance prediction was presented. In order to verify the accuracy of the simulation, the hydraulic performance was compared with the experiment data. Base on the result of the analysis in the Francis turbine, the following conclusions are drawn.

1. The simulation results by cavitating flow computation based on the mixture model agree well with experimental data.
2. With the decreasing of the cavitation coefficient, the pressure of the suction on the blade surface is decreasing gradually. And when the cavitation coefficient is lowed to a certain extent, the low-pressure area will appear the vapour area. And at the same cavitation coefficient, the vapour area at the optimum condition is largest.
3. With the decreasing of the cavitation coefficient, the vortex flow is appeared at the center of the draft tube inlet.

Acknowledgements

The research work was funded by National Science and technology support program (no.2013BAB08B03) and the National Natural Science Foundation of China (nos. 51276158).

References

[1] Kumar P, Saini R P 2010 Study of cavitation in hydro turbines—A review [J] *Renewable and Sustainable Energy Reviews*. **14(1)** 374-83.
[2] Srinivasan V, Abraham J S, Kozo S 2009 Numerical simulation of cavitation dynamics using a cavitation-induced-momentum-defect (CIMD) correction approach [J] *Applied Mathematical Modelling*. **33(3)** 1529-59.
[3] Zhao J, Wei Y, Zhang J et al 2009 Effect of various turbulence models on simulated results of cavitation flow [J] *Engineering Mechanics*. **8** 042.
[4] Wang Y, Wang B, Liu H 2014 Numerical simulation of sheet cavity shedding and cloud cavitation on a 2D hydrofoil *J. Chinese Journal of Hydrodynamics A*. **2** 006.
[5] Wu Y, Liu S 2011 Simulations of unsteady cavitating turbulent flow in a Francis turbine using the RANS method and the improved mixture model of two-phase flows [J] *Engineering with Computers*. **27(3)** 235-45.
[6] Nishi M, Liu S H 2013 An outlook on the draft-tube-surge study [J] *International Journal of Fluid Machinery and Systems*. **6(1)** 33-48.
[7] Menter F R, Kuntz M, Langtry R 2003 Ten years of Industrial Experience with the SST Turbulence Model [J] *Turbulence, Heat and Mass Transfer*. **4(1)**.